

Review

One-Dimensional Nanostructure Field-Effect Sensors for Gas Detection

Xiaoli Zhao †, Bin Cai †, Qingxin Tang *, Yanhong Tong * and Yichun Liu *

Key Laboratory of UV Light Emitting Materials and Technology under Ministry of Education, Northeast Normal University, Changchun 130024, China;

E-Mails: zhaoxiaoli19870220@163.com (X.Z.); atad2008@126.com (B.C.)

† These authors contributed equally to this work.

* Authors to whom correspondence should be addressed; E-Mails: tangqx@nenu.edu.cn (Q.T.); tongyh@nenu.edu.cn (Y.T.); ycliu@nenu.edu.cn (Y.L.); Tel./Fax: +86-431-8509-9873 (Q.T.).

Received: 18 June 2014; in revised form: 29 June 2014 / Accepted: 15 July 2014 /

Published: 31 July 2014

Abstract: Recently; one-dimensional (1D) nanostructure field-effect transistors (FETs) have attracted much attention because of their potential application in gas sensing. Micro/nanoscaled field-effect sensors combine the advantages of 1D nanostructures and the characteristic of field modulation. 1D nanostructures provide a large surface area-volume ratio; which is an outstanding advantage for gas sensors with high sensitivity and fast response. In addition; the nature of the single crystals is favorable for the studies of the response mechanism. On the other hand; one main merit of the field-effect sensors is to provide an extra gate electrode to realize the current modulation; so that the sensitivity can be dramatically enhanced by changing the conductivity when operating the sensors in the subthreshold regime. This article reviews the recent developments in the field of 1D nanostructure FET for gas detection. The sensor configuration; the performance as well as their sensing mechanism are evaluated.

Keywords: gas sensors; one-dimensional nanostructures; semiconductor; field-effect transistor

1. Introduction

Due to the excellent and well-known properties of one-dimensional (1D) nanoscaled materials, interest in 1D nanostructures, such as nanowires and nanotubes, for gas detection has increased substantially in recent years [1,2]. Compared with bulk materials, 1D nanostructures have obvious advantages for gas detection as follows: (i) High surface area-volume ratio. Gas sensors involve a surface response process, so a high surface area-volume ratio favors the adsorption of more gas molecules on the sensors and accelerates the charge accumulation, improving the sensitivity and response velocity [3]; (ii) High crystalline structure. Most 1D nanostructures are single crystals, which are free of defects and grain boundaries. The nature of the single crystal is favorable for the study of the sensing mechanism; (iii) Small dimensions. The nano/microscale size of 1D nanostructures can effectively decrease the sensor size, improve the integration level, decrease the power dissipation, and lower the cost.

Most 1D nanostructure gas sensors have applied semiconductors as the sensing material. The semiconductor sensor is one of the most common used gas sensors. They have advantages such as low cost, long duration, high sensitivity, and reliability, *etc.* The semiconductor materials were mainly focused on metal oxides, such as SnO₂, V₂O₅, WO₃ and TiO₂. Most of them operate with a two-terminal resistor mode. The field-effect transistor (FET) is another alternative device configuration for gas detection [4]. One key advantage of field-effect sensors over resistor sensors is the current modulation by the extra gate electrode [5]. The sensitivity can be dramatically enhanced by modulation of the gate electrode when operating the devices in the subthreshold regime. Besides the current, the multiple parameters, such as mobility, threshold voltage, and subthreshold slope, *etc.*, also can be used for sensing. The integration of the change of multiple parameters in the test ambient can realize the selectivity, which provides a way to overcome the challenges in gas identification for semiconductor sensors. The third advantage of the field-effect sensors is that the sensor response can be enhanced by combining them in oscillator and adaptive amplifier circuits [5]. Finally, field-effect sensors can operate at room temperature, which has advantages of low power consumption, long device lifetime, and reduced explosion hazards. These merits in field-effect sensors combined with the 1D single crystal nanostructures are therefore pushing the development of the 1D nanostructure field-effect sensors. Up to the present, a series of research works on the gas sensing behavior of 1D nanostructure field-effect sensors have been reported. Table 1 lists the performance of the reported 1D nanostructure field-effect sensors. Many kinds of materials were investigated as sensing materials for the detection of different gases, including In₂O₃, SnO₂, ZnO, CuO, carbon nanotubes (CNTs), Si, InAs, indolo[3,2-b]carbazole, 2,8-dichloro-5,11-dihexylindolo[3,2-b] carbazole (CHICZ) and CuPc. Among them, In₂O₃, SnO₂ and CNT are the most used materials. Resistor sensors generally are operated at high temperatures of 200–600 °C in order to achieve enhanced chemical reactivity between the sensing materials and the detected gases. In comparison, most of field-effect sensors can operate at room temperature, as shown in Table 1.

Table 1. The performance of reported 1D nanostructure field-effect sensors.

Material	NW/NB/N T ^b case	Operating Temperature (°C)	Target	LOD ^c	Sensitivity at LOD	Dimension (µm)	Response Time	Recover Time	Ref.
In ₂ O ₃	single	RT ^c	NO ₂	500 ppb	*	0.01	10~12 min	*	[3]
In ₂ O ₃	single	RT	NH ₃	0.02%	*	0.01	2 min	*	[3]
In ₂ O ₃	single	RT	NO ₂	20 ppb	25% ^g	0.01	*	*	[6]
In ₂ O ₃ :Zn	single	RT	CO	1 ppm	*	0.125	20 s	10 s	[7]
In ₂ O ₃ :Mg	single	RT	CO	500 ppb	$6.9 \times 10^{4\%}$ ^{1/f}	0.05	8 s	*	[8]
SnO ₂	single	100	H ₂	10 ppm	*	0.06	*	*	[9]
SnO ₂	single	RT	NO ₂	10 ppb	$7.16 \times 10^{5\%}$ ^f	~0.3	*	*	[10]
SnO ₂	single	250	H ₂ S	500 ppm	150% ^f	~0.56	*	*	[11]
SnO ₂	single	250	CO	100 ppm	*	~0.56	*	*	[11]
SnO ₂	single	250	CH ₄	100 ppm	*	~0.56	*	*	[11]
SnO ₂ :Sb	single	RT	ethanol	40 ppm	113% ^f	0.05~0.15	9 s	44 s	[12]
ZnO	single	RT	O ₂	10 ppm	64% ^g	0.06	*	*	[13]
ZnO	single	RT	NO ₂	200 ppb	*	*	*	*	[14]
CuO	single	200	CO	100 ppm	*	0.05~0.1	10 s	*	[15]
CNT	multiple	RT	NO ₂	100 ppt	80% ^g	0.002	*	*	[16]
CNT	single	RT	NO ₂	300 ppm	*	0.001	*	*	[17]
CNT	single	RT	NO ₂	40 ppm	3% ^f	*	*	*	[18]
CNT	multiple	RT	DPCP ^d	1 ppm	$10^{4\%}$ ^f	*	10 s	*	[19]
CNT	single	RT	NO ₂	2 ppm	*	~0.0014	300 s	*	[20]
CNT	single	RT	NH ₃	0.02%	*	~0.0014	600 s	*	[20]
Si	multiple	RT	NO ₂	20 ppb	13% ^g	0.018	*	*	[21]
InAs	single	RT	IPA	*	*	0.025	*	*	[22]
InAs	single	RT	acetone	*	*	0.025	*	*	[22]
InAs	single	RT	ethanol	*	*	0.025	*	*	[22]
InAs	single	RT	H ₂ O	*	*	0.025	*	*	[22]
CHICZ ^a	single	RT	ethanol	*	*	3~6	*	*	[23]
CuPc	single	RT	SO ₂	500 ppb	119% ^g	0.21	3 min	8 min	[5]

^a CHICZ: indolo[3,2-b]carbazole,2,8-dichloro-5,11-dihexylindolo[3,2-b] carbazole; ^b NW/NB/NT: Nanowire/Nanobelt/Nanotube; ^c RT: Room temperature; ^d DPCP: (diphenylchlorophosphate)IPA(Isopropyl Alcohol); ^e LOD: Limit of detection; ^f $S = P_g/P_a \times 100\%$; ^g $S = (P_g - P_a)/P_a \times 100\%$, P_g is the test signal of the sensor in the target gas, P_a is the test signal of the sensor in carrier gas.

The purpose of this article is to review recent developments in the field of 1D nanostructure FETs in gas sensing. The methods used to obtain the main performance parameters are presented. Four different research areas are reviewed: (i) Fundamentals of the gas sensors, which presents the basic principle of the 1D nanostructure field-effect sensors; (ii) Surface modification, which gives the most commonly used method for improved sensing performance by the functionalization of semiconductor nanowire or electrodes; (iii) Doping of nanowires, which optimizes the gas sensing by increasing the defects in nanostructures; (iv) New-type device configurations, which present new designs to improve the performance of the sensors. It is hoped that the examples presented here will encourage researchers to combine different materials or methods, or produce new designs that show improved or unique sensing properties.

2. Gas Sensor Performance Characteristics

Sensitivity, response time, recovery time and limit of detection (LOD) are typically reported as the main performance parameters of a 1D nanostructure field-effect sensor. The definition of the sensitivity is determined by comparing the test signal of the device before and after exposure (such as conductance, resistance, current, threshold voltage and mobility *etc.*). If the value of the test signal is decreased upon exposure to the target gas atmosphere, the sensitivity S is defined as P_a/P_g or $(P_g - P_a)/P_g$, where P_g is the test signal of the device in the target gas, and P_a is the original signal of the sensor. If the value of the test signal upon exposure to the target gas is increased, the sensitivity is defined as P_g/P_a or $(P_a - P_g)/P_a$. The response time (recovery time) is generally defined as the time period needed for the device to undergo a change from 10% to 90% (or from 90% to 10%) of the test signal value in equilibrium upon exposure to a target gas. In the reported literature, LOD is generally estimated by the lowest concentration of the device that can detect.

Selectivity is one of the most important parameters in gas sensors. According to the International Union of Pure and Applied Chemistry (IUPAC), the selectivity refers to the extent to which it can determine particular analytes under given conditions in mixtures or matrices, simple or complex, without interferences from other components [4]. As known to all, selectivity is one of the biggest challenges for semiconductor sensors, and so far the main efforts have been addressed to the detection of such analytes in solution [24]. One main detection mechanism of semiconductor sensor is based on the principle that the conductivity of the sensing material changes as a consequence of the interaction between the detected gas molecules and the surface complexes such as O^- , O^{2-} , H^+ and OH^- . The formed electron-depletion layer on the semiconductor surface decreases or increases the free carrier concentration of the material. This gives rise to the changed conductivity or threshold voltage. This process makes semiconductor sensors generally present a sensing response to all oxidizing and reducing gases. Some sensors show high sensitivity to only one analyte, which is referred to as specificity, with the 100% selectivity. To date, although some sensors are very sensitive to certain analytes, for example, NO_x , with LOD ranging from 10 to 200 ppb, they generally suffer from low selectivity or require elevated working temperatures [25].

3. Progress of Micro/Nanoscaled Single Crystals Field-Effect Sensors

Field-effect sensors have been known for more than four decades. In 1975, Lundstrom *et al.* reported the first field-effect sensors [26,27]. A 10-nm-thick palladium layer was used as gate electrode and Si was used as semiconductor for the detection of hydrogen. The threshold voltage of this transistor was changed with the partial pressure of hydrogen at ambient atmosphere. They proposed a model where hydrogen molecules were adsorbed on the palladium gate, and diffused into the Pd-SiO₂ interface forming a dipole layer. These hydrogen atoms changed the work function of the inner palladium surface and therefore affected the transistor threshold voltage.

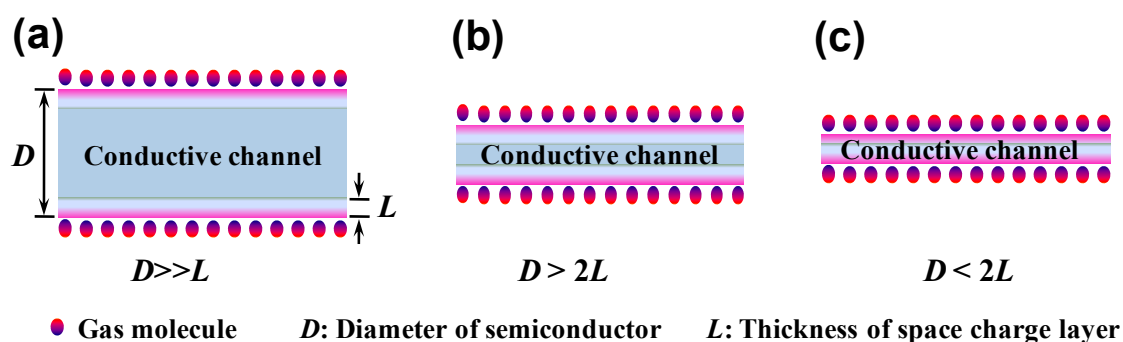
In 2000, Dai *et al.* first fabricated a field-effect sensor based on individual single-walled carbon nanotubes (SWNTs) [20]. The Ni/Au was used as source-drain electrodes and SiO₂ was used as the dielectric. The threshold voltage shifted towards to the negative direction of the gate voltage in NH₃ and shifted towards to the opposite direction in NO₂. Exposure to NH₃ for 10 min the conductance

decreased two orders of magnitude, while the conductance increased three orders of magnitude when the device was exposed to NO₂. They ascribed the dramatic conductance changes to the change of the relative location of the Fermi level of the nanotubes. Exposure of the device to NH₃ shifted the valence band away from the Fermi level, resulting in hole depletion and reduced conductance. Exposure to NO₂ resulted in the Fermi level shifting closer to the valence band, enriched hole carriers in the nanotube, and enhanced conductance. Since then, 1D nanostructure field-effect sensors have attracted researchers' attention, the related devices have been designed, and their work principles and sensing properties have been studied.

3.1. Fundamentals of Gas Sensors

The fundamental mechanism of the semiconductor sensors is still controversial. For the semiconductor resistor sensors, the changes in conductivity are believed to be related to the formation of a space charge layer at the semiconductor surface after gas adsorption. Therefore, the ratio of the thickness of the space charge layer to the conductive channel dimension determines the sensitivity of the sensor. The higher the surface area-volume ratio, the higher the dimension ratio of the space charge region to the conductive channel, as shown in Figure 1. This explains why the adsorption of the gas molecules on nanostructures can change the conductance more dramatically. The experimental results have confirmed that the sensitivity of the sensors based on nanowires or nanoparticles is far higher than that of bulk materials [28,29].

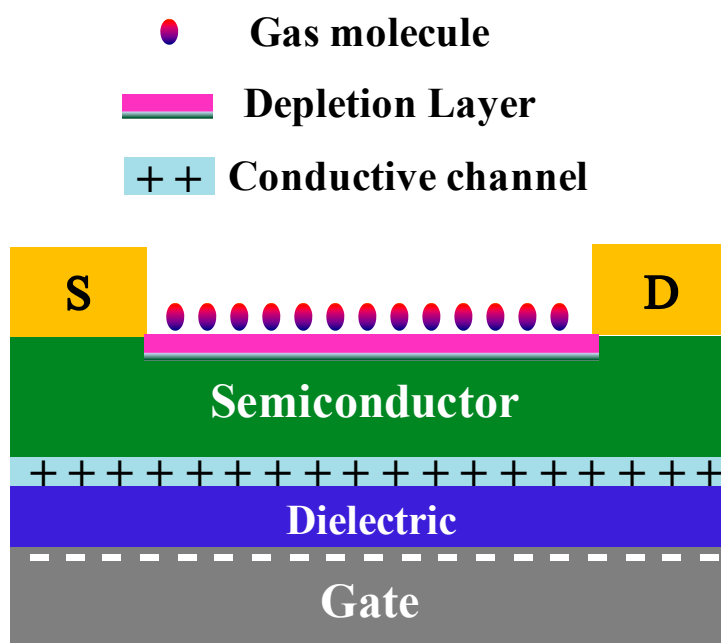
Figure 1. The relation between the thickness of semiconductor and the space charge layer for resistor sensor. (a) $D \gg L$; (b) $D > 2L$; (c) $D < 2L$, D : the diameter of the semiconductor; L : the thickness of the space charge layer.



For the response mechanism of the field-effect sensors, Torsi *et al.* proposed that the modulation effect of the gate electrode on the current magnified the sensor response signal [30]. Leeuw *et al.* have demonstrated the shift of the threshold voltage upon exposure to NO₂ with n-type, p-type, and ambipolar semiconductors [31]. They ascribed the response to gate bias-induced electron trapping [28,31]. Further, by delaminating the semiconductor with adhesive tape and measuring the surface potential of the gate dielectric by scanning Kelvin probe microscopy, they showed that the trapped electrons were located at the gate dielectric [32]. Although the work principle of the field-effect sensors is controversial, it is believed that the effect of the space charge layer formed by gas adsorption on the conductive channel plays a key role. Frisble *et al.* have carried out atomic force microscope (AFM) measurements,

and have confirmed that the gate voltage concentrated the conductive channel in one molecular layer at the interface between the semiconductor and dielectric [33]. On the other hand, Yamazoe *et al.* confirmed that the thickness of the space charge layer caused by gas adsorption was about a few nanometers [29]. Therefore, the size of the conductive channel is comparative to the thickness of the space charge layer in FET, as shown in Figure 2. In this case, the sensitivity of the device can be improved dramatically. For example, the reported the lowest LOD of the individual In_2O_3 resistor sensor is 500 ppb at the operating temperature of 400 °C [34], while the lowest LOD of the In_2O_3 field-effect sensor is 20 ppb at room temperature [6]. Tang *et al.* [10] recently reported that their SnO_2 nanobelt field-effect sensors with the traditional metal electrodes indicated the sensitivity of $5.48 \times 10^7\%$ at 50 ppb NO_2 , which was four orders higher than the reported highest resistor SnO_2 nanobelt sensor (1900% at 100 ppb) [35], showing the dramatic effect of the gate electrode in improving the sensitivity [10]. Lu *et al.* showed that the sensitivity to oxygen of the ZnO nanowire field-effect sensor was higher with smaller-radius nanowires [13]. Moreover, the oxygen detection sensitivity could be modulated by the gate voltage. They ascribed the gate-dependence detection sensitivity to the gate modulated electron concentration in the nanowire channels. When the gate voltage is far above the threshold so that the modulation effect of the gate on the current is weak, the electron concentration in the channel is very high and the gas molecules adsorbed on the 1D nanostructure captured only a small portion of the available carriers, therefore, the relative conductance change is very small. However, when the device operates in the subthreshold regime and the FET is gated just above the threshold, the channel carriers are substantially depleted and the conductance change caused by gas adsorption becomes much more significant. This results in a high sensitivity for 1D nanostructure field-effect sensors.

Figure 2. Schematic image of the interaction of the adsorbed gas molecules with FET.



As we know, most 1D nanostructure field-effect sensors work in room temperature, which makes them hardly reversible and leads to long recovery times, since the activation energy for desorption is

generally higher than the thermal energy. A few research groups have demonstrated novel methods to shorten the recovery time. For example, Yang *et al.* illuminated a SnO₂ nanobelt device with ultraviolet (UV) light of energy near the SnO₂ band gap [36]. They found that the photogenerated carriers accelerated the desorption velocity of device on NO₂. Lu *et al.* applied a strong negative field to refresh the ZnO nanowire field-effect sensors by an electrodesorption mechanism [14]. They proposed that a negative gate potential possibly depleted the electrons in the nanowire and reduced the number of electrons available at vacancy sites, thus lowering the chemisorption rate. The negative field drove the holes to migrate onto the surface, resulting in the discharge of gas molecules. In addition, the negative gate induced repulsive field stretches and weakened the bonding between these adatoms and adsorption sites. Yoo *et al.* applied a negative gate voltage pulse in NO₂ and a positive gate voltage pulse in NH₃ to refresh CNT field-effect sensors [17]. The NO₂ molecules were physically adsorbed onto the CNT via dipole interactions, and electrons were transferred from the CNT to NO₂ molecules. Therefore, they proposed that the negative gate voltage induced the repulsive force, which may weaken the binding between the CNT and NO₂ molecules and accelerate their desorption.

3.2. Surface Modification

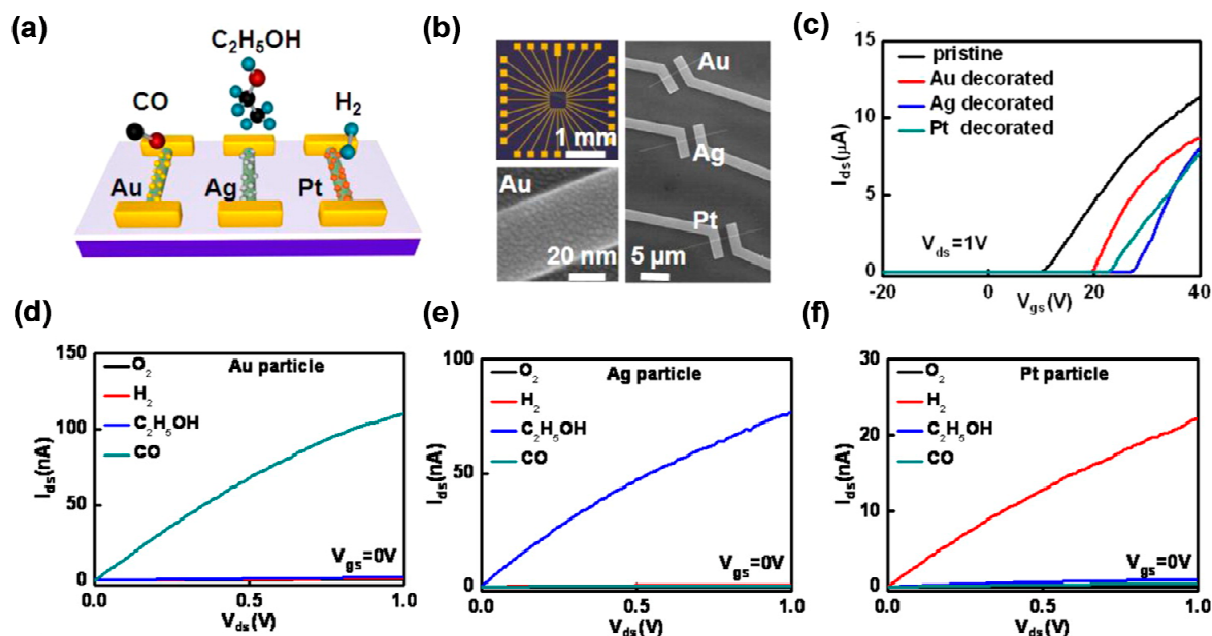
3.2.1. Modification of Metallic Nanoparticles on Semiconductor Nanowires

Modification of metallic nanoparticles on semiconductor nanowire/nanobelt/nanotubes is the most commonly used way to improve the sensor performance for both the resistor sensors and field-effect sensors [37–45]. Noble metals, such as Pt, Ag, Pd, Au, *etc.*, are generally used as highly-effective oxidation catalysts to enhance the catalytic activity of gas sensors. Two mechanisms are considered when the 1D nanostructures are modified with metallic nanoparticles [46]. One is that the nanoparticles on the nanowire surface create the Schottky barrier-type junctions within the nanowire, resulting in the formation of electron depletion regions. The other mechanism is a “back-spillover effect”, which is a purely chemical catalytic effect when the metallic nanoparticles are dispersed on the surface of 1D nanostructures. Moskovits *et al.* compared the sensing performance of individual SnO₂ nanowire and nanobelt gas sensors before and after functionalization of the Pd nanoparticles [46]. Pd catalyst particles were deposited *in situ* in the same reaction chamber where the sensing measurements were carried out. The *in situ* deposition and sensing characterization ensured that the observed change of sensing performance was due to the Pd functionalization rather than any variation in properties from one nanowire to another. The effect of metal deposition on the nanowire conductance was monitored throughout the deposition process by continuously measuring I_{SD} . High resolution transmission electron microscopy (HRTEM) images confirmed that no bulk oxidation occurred for these Pd nanoparticles. Upon exposure to O₂ and H₂, the device showed the increased I_{SD} . The Pd functionalized nanowire devices showed dramatically improved sensitivity and response speed, which was ascribed to the enhanced catalytic dissociation of the molecular adsorbate on the Pd nanoparticle surfaces and the subsequent diffusion of the resultant atomic species to the oxide surface.

Another obvious advantage of functionalizing semiconductor nanowires with catalytically active metals is to achieve selectivity for gas sensors. Currently, the development of highly selective devices remains a challenge for semiconductor sensors. It has been found that the devices functionalized with

different metal nanoparticles show different response characteristics to different gases [45,47–49]. Ho *et al.* used Mg-doped In_2O_3 nanowire enhanced-mode field-effect sensor arrays decorated with various discrete metal nanoparticles (*i.e.*, Au, Ag and Pt), to selectively distinguish among three reducing gases (e.g., CO, $\text{C}_2\text{H}_5\text{OH}$ and H_2), with high sensitivity [8]. The deep enhanced-mode FET could not detect the reducing or oxidizing gases, which provided an ideal platform to introduce the gas selectivity and sensitivity into the nanowire surface by decorating various metal nanoparticles. The schematic, optical, and scanning electron microscope (SEM) images of the Au, Ag and Pt decorated nanowire field-effect sensors are shown in Figure 3a,b. Figure 3c presents the $I_{SD}-V_{GS}$ curves for the sensors with and without the metal modification. Four target gases, O_2 , H_2 , $\text{C}_2\text{H}_5\text{OH}$ and CO, were added to the continuously flowing air stream at a low concentration of 100 ppm, respectively. Each type of metal nanoparticle could respond to a specific gas molecule through different catalytic reactions. Figures 3d–f present the $I_{SD}-V_{SD}$ characteristics for Au, Ag and Pt-decorated FETs. The gas specific enhancement in the FET conductance was clearly demonstrated with Au, Ag and Pt nanoparticle- decorated nanowire channels for the selective detection of CO, $\text{C}_2\text{H}_5\text{OH}$ and H_2 , respectively.

Figure 3. (a) Schematic of the sensor arrays. The surface of nanowires was decorated with Au, Ag, and Pt nanoparticles, respectively; (b) Optical (top left) and SEM (right) image of the chemical sensor arrays. High magnification SEM (bottom left) image of Au decorated Mg-doped In_2O_3 nanowire; (c) The transfer curves for the sensors with and without the metal decoration; (d–f) The output curves for Au, Ag and Pt decorated enhanced-mode FETs toward the gas specific detection of O_2 , H_2 , $\text{C}_2\text{H}_5\text{OH}$, and CO [8].

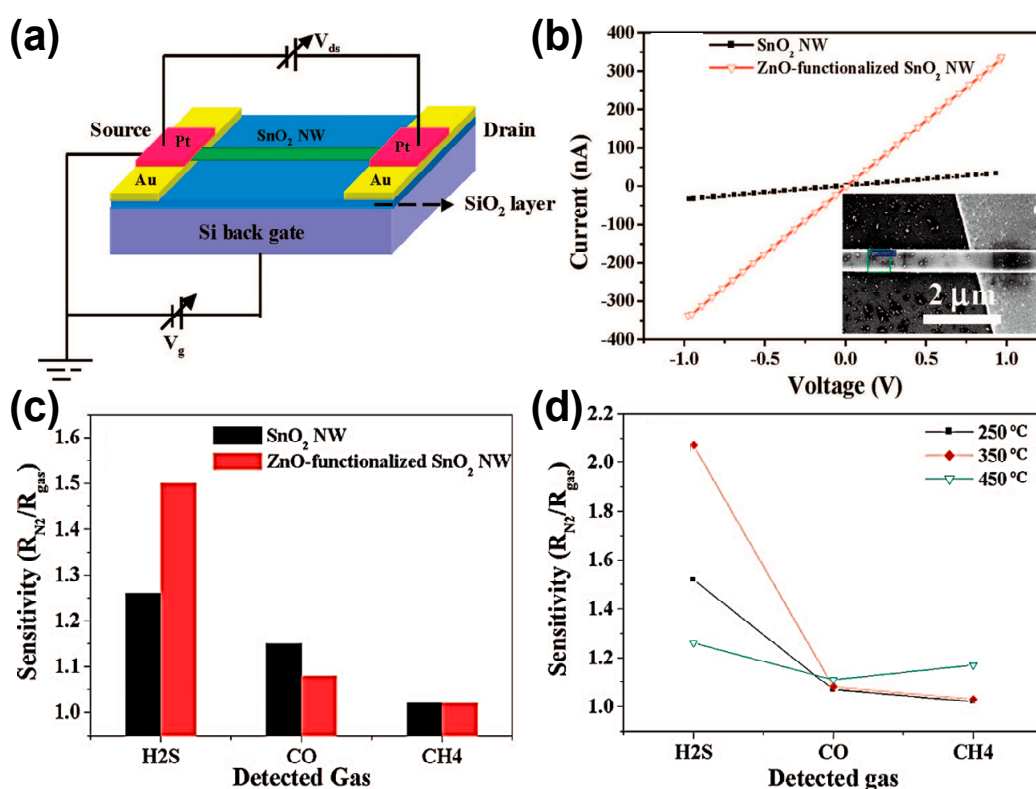


3.2.2. Modification of Semiconductor Nanoparticles on Semiconductor Nanowires

As discussed above, surface modification is an effective method in improving sensing performance. Wang *et al.* improved the sensing properties of the SnO_2 nanowire sensors by modification of ZnO nanoparticles. The 10-nm-thickness ZnO nanoparticles were deposited on the surface of SnO_2 nanowires via magnetron sputtering [11]. Figure 4a is the schematic image of the device. Figure 4b

shows the I - V curves of the single SnO₂ device before and after ZnO deposition. The conductivity of SnO₂ nanowire increased dramatically when the nanowire surface was modified with ZnO nanoparticles. Figure 4c shows the sensitivities of a SnO₂ nanowire sensor to three detected gases (500 ppm H₂S, CO, and CH₄) before and after ZnO modification. It was found that the sensitivity changes were different for different gases after ZnO surface modification. After the SnO₂ nanowire was modified with ZnO nanoparticles, the sensitivity of the device increased for H₂S, while the sensitivity decreased for CO, and was almost unchanged for CH₄. These results showed that the selectivity of the single SnO₂ nanowire was improved to a certain extent by surface functionalization. Figure 4d shows the different sensitivity of the ZnO nanoparticle-modified SnO₂ nanowire sensor at different operation temperatures upon exposure to different gases. By operating the devices at the optimized temperature, the sensitivity and selectivity of the device could be effectively improved. The device showed the highest sensitivity to H₂S at 350 °C and to CH₄ at 450 °C. They proposed that the formation of n-n heterojunction with an energy difference of about 0.75 eV between ZnO and SnO₂ possibly was responsible for the enhanced selectivity [50]. At the same time the coordinate effect of two sensing materials also played a key role.

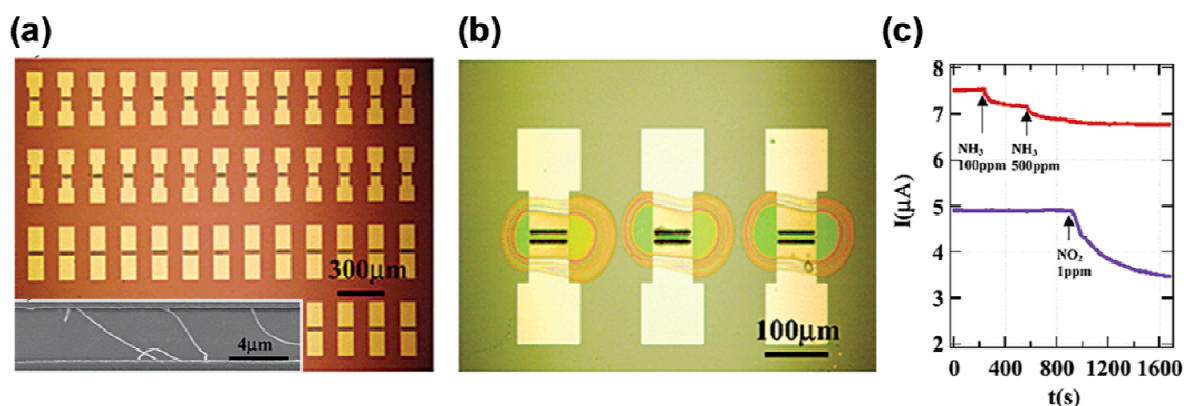
Figure 4. (a) Schematic illustration of a single SnO₂ nanowire-based FET; (b) I - V curves of the single SnO₂ nanowire device before and after ZnO deposition. The inset is the corresponding SEM image of the single SnO₂ nanowire device after ZnO deposition; (c) Comparison of gas-sensing sensitivity of the pure and ZnO-functionalized SnO₂ nanowire sensor to three detected gases; (d) Sensitivity to three detected gases of the ZnO-functionalized SnO₂ nanowire sensor at different operation temperatures. The concentration of detected gases was 500 ppm, the operation temperature was 250 °C, and the fixed bias was 1 V [11].



3.2.3. Modification of Organic Molecules on Semiconductor Nanowires

Another effective method for the realization of selectivity is to modify the semiconductor with organic molecules. One way is to functionalize each semiconductor element in an array of sensors with different organic molecules, for example, polymers or silanes. Dai *et al.* functionalized multiple-nanotube array devices with two different polymers, polyethyleneimine (PEI) and Nafion, by microspotting the different solutions to position the pin over each individual device [16]. This method allowed the assembly of multiple devices could selectively detect NO_2 and NH_3 in gas mixtures. The morphology of the multiple-SWNT device array, a single device, and the devices after microspotting, are shown in Figure 5a,b. The PEI contains high-density amines, and renders as-grown SWNTs electron rich, and hence is high selective toward strongly electron-withdrawing molecules. Nafion is a polymer with a Teflon backbone and sulfonic acid side groups. It is sensitive to NH_3 that tends to react with H_2O in the environment to form NH_4OH . As shown in Figure 5c, the Nafion-functionalized device presented a decrease of the conductance in 100 and 500 ppm NH_3 due to NH_3 electron donation to the p-type device reducing the majority hole carriers, while a PEI-functionalized device on the same chip did not show any response to NH_3 . When introducing 1 ppm of NO_2 into the environment in 500 ppm NH_3 , the Nafion-functionalized device did not respond, while the PEI-functionalized device showed a decrease of the conductance. These results clearly demonstrated that multiplexed nanotube sensor arrays are promising for specific molecular detection in complex chemical environments.

Figure 5. (a) Optical image of an array of multiple-SWNT devices. The inset is SEM image of several nanotubes bridging two opposing Mo electrodes in a device; (b) Optical image showing three multiple-tube (MT) devices after microspotting with droplets of polymer solutions; (c) Red (top) curve: a device coated with Nafion exhibited a response to 100 and 500 ppm of NH_3 in air, and no response when 1 ppm of NO_2 was introduced to the environment. Blue (bottom) curve: a PEI-coated device exhibiting no response to 100 and 500 ppm of NH_3 and large conductance decrease for 1 ppm of NO_2 [16].



Heath *et al.* selectively detected hexane and acetone vapor by modification of Si nanowires on a sensor array [21]. The Si nanowire was naturally coated by a layer of SiO_2 , which is easily modified by a lot of commercially available reagent molecules that contain silanes. They left one device unmodified, and the other three devices were chemically modified by alkane-, aldehyde- and amino-silanes using a vapor deposition method. The sensor array was fabricated as a field-effect configuration, while

the gate voltage was not applied when the different gases were detected. All devices presented an increase of the conductance upon exposure to two different gases, while the magnitude of the response was different for each device that was determined by the surface chemistry.

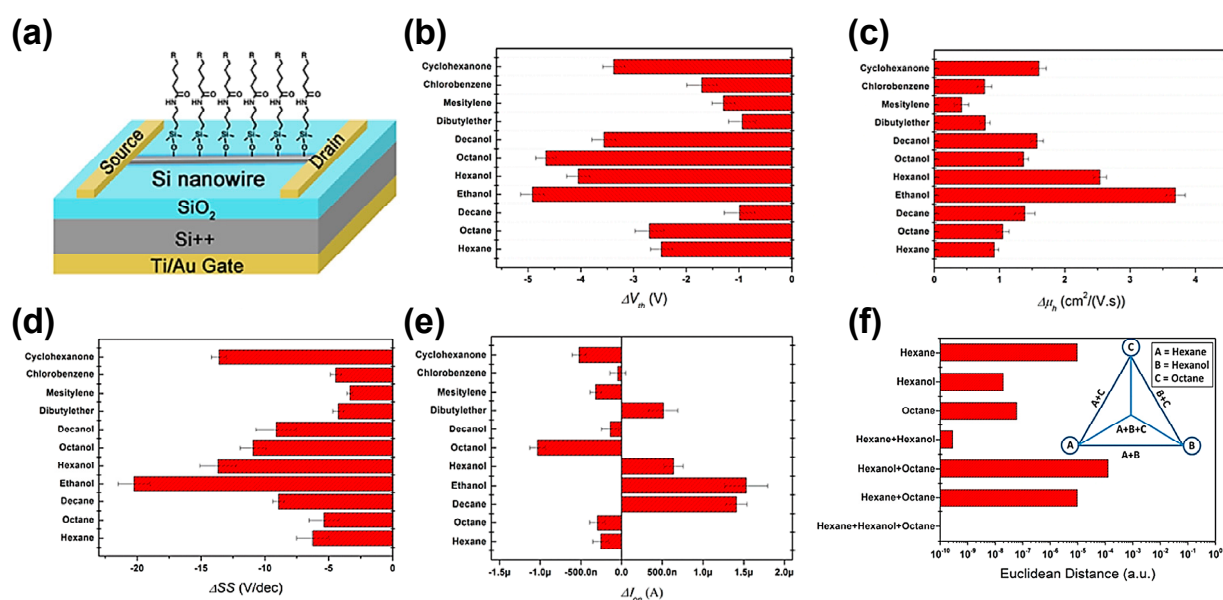
The detection of nonpolar analytes with Si nanowire FETs remains challenging under real-world conditions. The Haick group have used tailor-made organic functionalized Si nanowire FETs and recorded the electrical response of sensors with high signal-to-noise ratios upon exposure to nonpolar analytes [51,52]. They attributed the detection of the nonpolar analytes to two indirect effects: (i) a change in the dielectric medium close to the Si nanowire surface; (ii) a change in the charged surface states at the functionality of the Si nanowire surface. The results provided clear evidence for the leading role of molecular gating in detecting nonpolar analytes and a launching pad for real-world sensing applications with Si nanowire FETs.

The “hysteresis” phenomenon of the Si nanowire FETs is generated by interactive effects [53], such as the periphery surfaces, interfaces and/or adsorbed atmosphere molecules near the charge carrier channel, which limits their performance under real-world conditions. To suppress this phenomenon, Haick *et al.* have used a series of systematically changed trichlorosilane-based organic monolayers to study the interactive effect of hysteresis and surface chemistry on a Si nanowire FET gas sensor [54]. The findings could extend the use of gated silicon nanowire gas sensors for discrimination between polar and nonpolar analytes in complex, real-world gas mixtures.

Although the selectivity can be improved by modifying the sensor array with different molecules or metal nanoparticles, the increased sensor number increases the power consumption and integrated size, complicating the device computation. Haick and his colleagues have used molecularly modified Si nanowire FETs to distinguish different polar and nonpolar volatile organic compounds (VOCs) in an atmosphere with background humidity (relative humidity: 40%) [55]. The combination of nanowire FET arrays has the best discriminative power between the various VOCs. Very recently, Haick *et al.* also used the multiple independent parameters of a specific molecularly modified Si nanowire FET as input for selective detection of specific VOCs [56]. Figure 6b–e presents the responses of a molecularly modified Si nanowire field-effect sensor on exposure to eleven VOCs at VOC concentration of $p_a/p_o = 0.08$ (where p_a and p_o are the VOC's partial pressure and vapor pressure, respectively, at a given temperature). The sensor exhibited negative responses in the threshold voltage V_{th} and the SS , while it showed positive responses in μ_h to all tested VOCs. In the I_{on} response plot, the sensor functionalized with the molecule containing the COOH functional group showed positive responses to decane, ethanol, hexanol, and dibutyl ether, and negative responses to the rest of the VOCs. These multiple sensing responses by one molecularly modified Si nanowire FET created a fingerprint for each VOC, which could be used for VOC discrimination. They selected four sensing parameters, including V_{th} , μ_h , I_{on} , and SS , and employed artificial neural network (ANN) models to seek selectivity towards specific VOCs. The selectivity depended on the difference in the combination of the four sensing parameters analyzed. Figure 6f shows the Euclidean distance (ED) of ANN outputs. The ED is the distance between the target vector and prediction vector, which can be used to evaluate the recognition power of the sensors. The ED values of all tested samples were below 10^{-3} . By a combination of multiple parameters from one Si nanowire field-effect sensor and ANN model, each of the VOCs in the tested mixture was perfectly identified. More important, the trained ANN model successfully predicted if a certain VOC existed in a binary and even ternary VOC mixture. They also

explored the effect of the functional groups and the chain length on the sensing properties of VOCs [57,58]. The change of the threshold voltage increased with the chain length of the molecular modification, while the change of relative hole mobility did not exhibit any obvious dependence on the chain length. They proposed that the electron-donating/withdrawing properties of the functional groups controlled the dipole moment orientation of the adsorbed VOCs. At the same time, the type of functional groups determined the diffusion of VOCs into the molecular layer.

Figure 6. (a) Scheme of a molecularly modified Si nanowire field-effect sensor; (b–e) Changes in V_{th} , μ_h , SS , and I_{on} of an electron-donating sensor on exposure to various VOCs at concentration of $p_a/p_o = 0.08$; (f) Euclidean distance of ANN outputs using an electron-withdrawing sensor to identify hexane, hexanol, octane and their binary and ternary mixtures. Inset: Schematics of the relationship among single VOCs and their binary and ternary mixtures in ANN outputs [56].

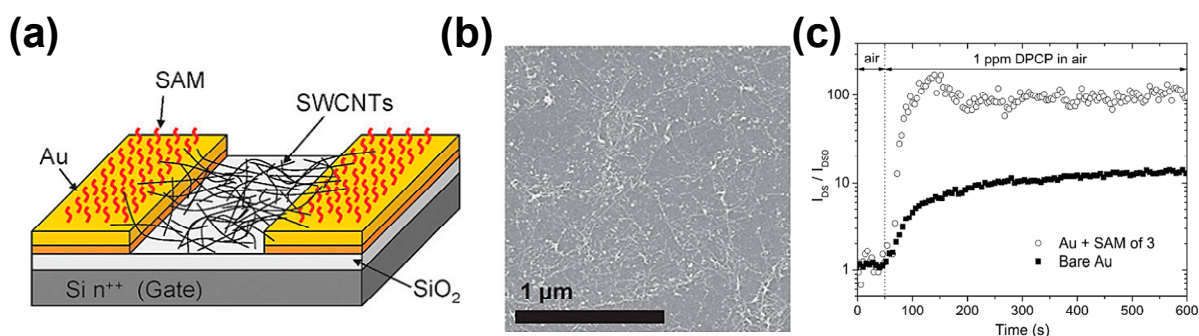


3.2.4. Assembly of Molecular Layer on Electrodes

Carella *et al.* applied a self-assembled monolayer (SAM) of organophosphorus (OP) compound- sensitive molecules to functionalize the electrode of a CNT network field-effect sensor [19]. The device was fabricated with bottom gate/bottom contact geometry. Ti/Au electrodes were prepared on a Si/SiO₂ substrate, and the functionalization was carried out by immersing the gold surface overnight in a freshly prepared 0.7 mM solution of acetone at room temperature. The schematic image of the device and the SEM image of the SWNT network are shown in Figure 7a,b. The response of CNT FET devices as a function of time at optimized V_{GS} before and after the functionalized of gold electrodes is shown in Figure 7c. The experimental results showed that the response of CNT FET to diphenylchlorophosphate/isopropyl alcohol (DPCP/IPA) vapors was highly improved after gold electrode functionalization. Pristine CNT field-effect sensors exhibited an increase of the current by a factor of ~ 13 , while the functionalized sensor showed a dramatically increased current by a factor ~ 100 . They ascribed the obviously improved response to the increased change of the Schottky barrier height at the interface between the electrode and the semiconductor after DPCP exposure, resulting in

the changed the work function of the gold electrode and hence higher sensitivity for the gold electrode functionalized device. The increased Schottky barrier for holes after the gold electrode functionalization was confirmed by the decreased “ON” current, and Kelvin probe force microscopy measurements.

Figure 7. (a) Schematic structure of the CNT FET with functionalized gold electrodes; (b) SEM image of the SWCNT network; (c) Normalized response to the CNT field-effect sensors upon exposure to DPCP vapors with bare and functionalized Au electrodes [19].

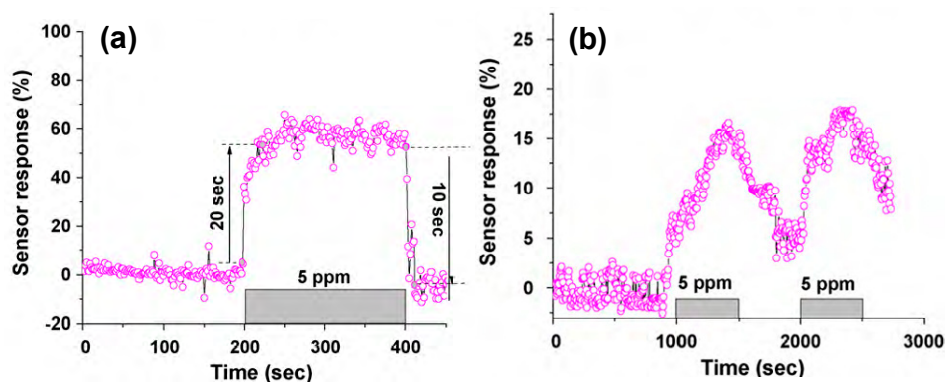


3.3. Doping of Nanowires

Doping metal oxide semiconducting nanowires is an effective strategy to improve the sensing performance. Lee *et al.* demonstrated a Zn doped In_2O_3 nanowire field-effect sensor for room-temperature detection of CO gas (Figure 8) [7]. The sensor was fabricated using 60 nm SiN_x as dielectric layer, Si as bottom gate electrode, and Cr/Au (10/50 nm) as source and drain electrodes. A good selectivity for CO gas over NO and NO_2 could be achieved. The sensitivity of the Zn doped In_2O_3 nanowire sensor was found to be almost three times higher than that of the undoped nanowire sensor. The response and recovery times for the Zn doped In_2O_3 nanowires sensor were 20 and 10 s, respectively, which was obviously higher than those of the undoped nanowire sensor. They ascribed the enhanced sensing performance to the increase of the defect number and the modification of the Fermi level by doping. The electrical detection of the chemical species was dependent on the surface reactions between the nanowires and the chemical molecules. Most of the defects behaved as preferential adsorption sites for a gas molecule [59]. The doping induced defects improved the adsorption of gas molecules on the nanowire surface. On the other hand, doping changed the position of Fermi level of semiconductor in the energy band diagram which governed the electronic transportation between gas molecule and nanowire material. The chemical potential gradient between the adsorbed CO molecule and the nanowire was increased. This accelerated more electron transfer to reach equilibrium and therefore the faster sensor response output with higher sensitivity were obtained.

In general, SnO_2 behaves as n-type semiconductor. Wu *et al.* fabricated p-type SnO_2 nanowires by doping Sb [12]. Gas sensing experiments were conducted at room temperature by recording the I - V characteristics while applying a constant bias of 5 V. The doped nanowire device showed a rapid increased conductance as the device was exposed to the ethanol gas. The LOD reached 40 ppm. The response time was only ~ 8.3 s for the different ethanol concentrations. The recovery time was increased from 44 to 87 s with the increased ethanol concentration in the range of 40–300 ppm. The far faster response time than the recovery time ascribed to the much lower diffusion rate of gas molecules than the charge separation rate of electron-hole pairs.

Figure 8. (a) Sensor response plot of the Zn-In₂O₃ nanowire sensor for single cycle of 5 ppm CO gas; (b) Response plot for the undoped In₂O₃ nanowire-FET, when exposed to 5 ppm CO gas in two cycles [7].



3.4. New-Type Device Configuration

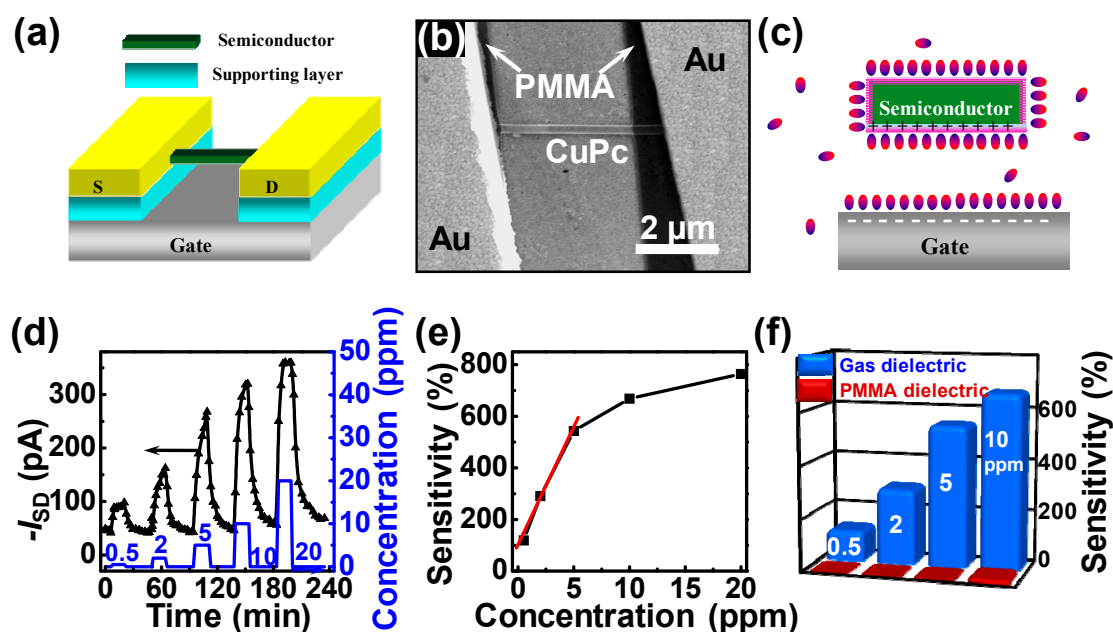
3.4.1. Gas as Dielectric

As mentioned in Section 3.1, in resistor sensors, the current passes through the whole semiconductor section which acts as the conductive channel. However, the conductive channel of the FETs is located in a few molecular layers at the interface between the semiconductor and the dielectric. Therefore, the gas adsorption in the conductive channel of FETs has a far larger influence than on the upper and side surface of the semiconductor layer. Further, for the traditional solid dielectric field-effect sensor, the conductive channel is capped by the semiconductor layer and the solid dielectric, and the gas molecules mainly adsorb to the upper and the two side surfaces of semiconductor (Figure 2). In contrast, the gas dielectric makes the conductive channel exposed to the detected gas (as shown in Figure 9c), which facilitates the direct interaction between the gas molecules and the conductive channel resulting in the improvement of the sensing performance.

Tang *et al.* demonstrated a gas dielectric field-effect sensor, where CuPc nanowire was used as semiconductor [5]. This is the first demonstration of SO₂ gas sensing based on organic FETs. Figure 9a,b are the schematic and SEM images of the device. The individual CuPc nanowire bridged on the supporting layer, and the Au films were stamped on the side of the CuPc nanowire to form the source and drain electrodes. Their experiment results showed that the gas dielectric field-effect sensor presented excellent parameters such as sensitivity, LOD, response time, recovery time, resolution, and operating temperature. Some of them were comparable to the commercialized solid electrolyte sensors. Figure 9d,e present the current response and the sensitivity in different SO₂ concentrations. The sensor was operated at room temperature. The LOD decreased over one order of magnitude (from 10 to 0.5 ppm) when the device configuration was changed from solid to gas dielectric. The LOD of gas dielectric sensor was 0.5 ppm with high sensitivity (119%) and high resolution (100 ppb), which is in a class with the highest detection limit for the semiconductor SO₂ sensors reported so far. The gas dielectric sensor showed the sensitivity of about 800% in 30 ppm SO₂, while the sensitivity of the solid dielectric sensor was only about 40% in the same SO₂ concentration. The histogram in Figure 9f clearly presents the dramatically improved sensitivity in different SO₂ concentration when the dielectric was changed from

solid to gas state. The response and recovery times of the gas dielectric device in 0.5 ppm SO₂ were only 3 and 8 min, respectively. The sensitivity showed the linear dependence on the concentration from 0.5 to 5 ppm with the change of 20% per 100 ppb SO₂, corresponding to a concentration resolution of 100 ppb. It showed that the device was applicability for the detection of low-concentration SO₂. The linear sensitivity dependence of Figure 9e in the low concentration (0–5 ppm) also showed the notable merits of the sensors for quantitative detection, direct electrical readout, and simplified device calibration process and auxiliary circuitry.

Figure 9. (a,b) The schematic and SEM images of gas dielectric FETs based on CuPc nanowire; (c) Schematic image for the work principle of gas dielectric sensor; (d) Real-time I_{SD} change of device to various SO₂ concentration (0.5, 2, 5, 10 and 20 ppm) at $V_G = -10$ V and $V_{SD} = -15$ V at room temperature. The blue line corresponds to SO₂ concentration (right y-axis); (e) Sensitivity of device as a function of SO₂ concentration at $V_G = -10$ V and $V_{SD} = -15$ V at room temperature. The red line is the linear fitting result in low-concentration SO₂; (f) Comparison of the gas sensitivity of gas dielectric (blue) and PMMA dielectric (red) devices in different SO₂ concentration (0.5, 2, 5 and 10 ppm) [5].

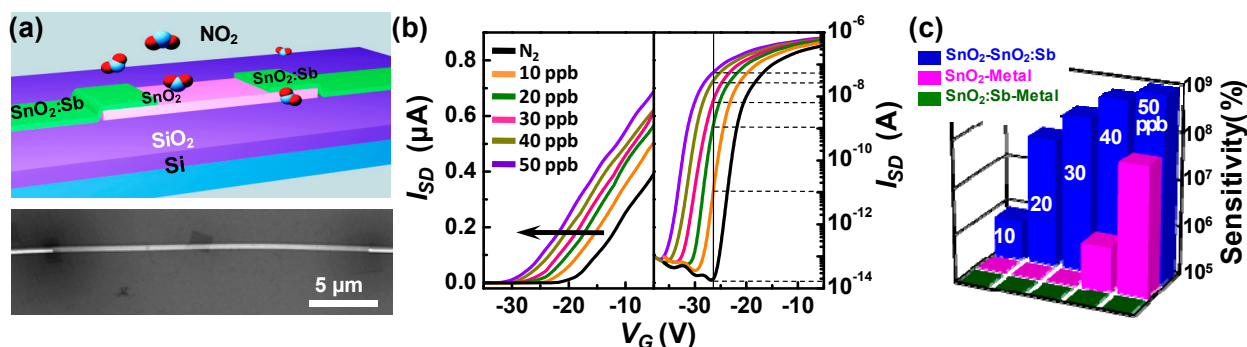


3.4.2. Conductive Nanowires as Electrodes

The contact interface between the electrodes and the semiconductor also plays an important role in gas sensing. Barbara *et al.* found that the response was delayed when the CNT/electrode contacts were covered with a thick and long passivation layer [18]. Tang *et al.* employed a novel design, by introducing the high-conductivity SnO₂:Sb nanobelts as electrodes, to fabricate the SnO₂ nanobelt field-effect sensors [10]. Figure 10a shows the schematic and SEM images of the device. The SnO₂:Sb nanobelt has the low resistivity (10^{-2} – 10^{-4} Ω·cm) and hence are capable to serve as the source and drain electrodes of the field-effect nanosensor. The good energy level matching of SnO₂:Sb with SnO₂ are also favorable for the carrier injection. The comparable size of the electrodes to the semiconductor also showed the potential application in nanoelectronics. Figure 10b is the transfer curves of the device

for different NO₂ concentrations. The LOD was shown to reach the ppb level (10 ppb), while maintaining both high sensitivity ($7.16 \times 10^5\%$) and high resolution (-3.2 V per 10 ppb). Sensitivity value was as high as $1.92 \times 10^8\%$ for NO₂ at 30 ppb, which was six orders of magnitude higher than the previously reported highest sensitivity, for concentration below the 50 ppb level. In addition, the V_T presented the linear dependence with the NO₂ concentration. The LOD, sensitivity and resolution of the sensors were even superior to the commercially available MiCS-2714 metal oxide sensor (30% at 50 ppb) [60].

Figure 10. (a) Schematic and SEM image of the SnO₂ nanobelt field-effect gas sensor with SnO₂:Sb nanobelts as electrodes; (b) Transfer characteristics of the device to various NO₂ concentrations (0, 10, 20, 30, 40 and 50 ppb) at room temperature; (c) Comparison of the sensitivity of the devices for different NO₂ concentrations (10, 20, 30, 40 and 50 ppb): SnO₂:Sb nanobelt with metal electrodes (green), SnO₂ nanobelt FET with metal electrodes (red), and SnO₂ nanobelt FET with SnO₂:Sb electrodes (blue) [10].



In their experiments, the transfer curves shifted towards the negative direction upon exposure to NO₂, as shown in Figure 10b. Such a change suggested a sensing mechanism different from that of the extensively reported semiconductor sensors. They further measured the sensing performance of the SnO₂ nanobelt field-effect sensor with the metal electrodes, and SnO₂:Sb nanobelt resistor sensor with the metal electrodes. The comparative results are presented in Figure 10c. The SnO₂:Sb nanobelt did not respond to NO₂ in the concentration range of 10–50 ppb. The field-effect sensor with metal electrodes showed a sensitivity almost four orders of magnitude lower than the field-effect device with SnO₂:Sb nanobelt electrodes in 10 ppb NO₂. These comparative experiments showed that the interface between the SnO₂ nanobelt and SnO₂:Sb nanobelt electrodes was responsible for the sensing of devices to NO₂.

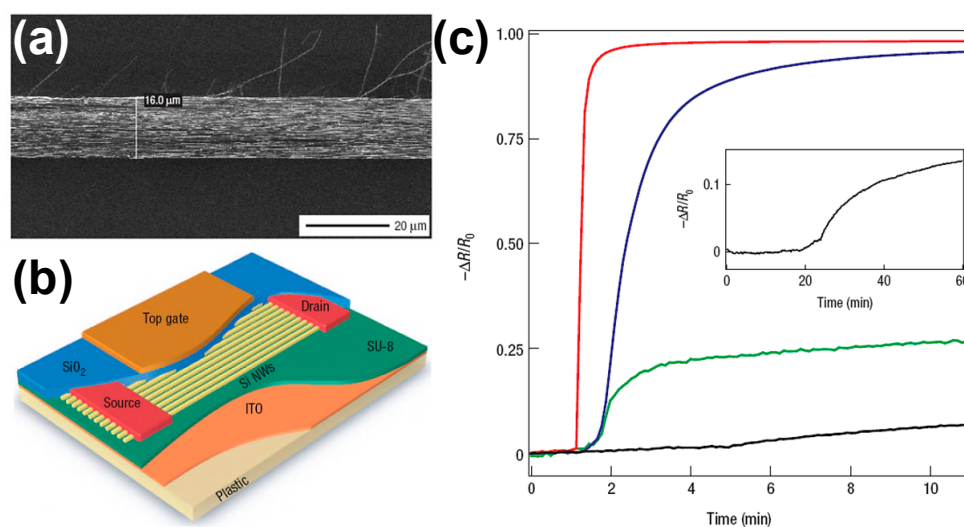
3.4.3. Nanowires Array as Semiconductor Layer

Multiple-nanowires or tube arrays as semiconductor layers of field-effect sensors accumulate the responses of the multiple wires, and hence are sensitive for gas detection. The multi-nanowire or tube averaging makes the electrical noise of the sensor far lower than that of the individual nanostructure device since the noise scales as $1/N$ (N is the number of tubes) [16,21]. Highly order and parallel array are requisite since the intersected network structure generally causes failed measurements in the field-effect properties due to the poor interface contact between semiconductor and dielectric.

Dai *et al.* employed a multiple CNT array as the semiconductor layer of a field-effect sensor [16]. The SWNT array was grown from the micropatterned catalyst on the preprepared Mo source and drain electrodes by chemical vapor deposition. The SWNT could adhere well onto the substrate surface. The average number of SWNTs across the electrodes for the single device was ~ 20 – 30 . Such a device has many advantages such as simple fabrication method, high yield, good electrical stability with low noise, and highly sensitivity. The individual nanotubes presented over 10% fluctuation of the conductance with time while the array device only showed $\sim 1\%$ fluctuation. The electrical conductance of a typical MT device increased by 80% when was exposed to 100 ppb of NO_2 in Ar.

Heath *et al.* selected a Si nanowire array as the semiconductor layer for field-effect sensors [21]. The morphology of the nanowire array is shown in Figure 11a. Figure 11b is the schematic image of the nanowire array sensor. One of main advantages for Si nanowires is the precise control over the dopant type and concentration. The devices were fabricated on a bendable flexible plastic substrate. Figure 11c shows the normalized response of a nanowire sensing element to NO_2 at different concentrations. The device exhibited sensitivities comparable to the best nanotube and metal-oxide nanowire devices on Si substrates [6,16,61]. The current increased $\sim 3000\%$ after 20 ppm NO_2 was introduced in N_2 for 1.25 min. The LOD was at least 20 ppb of NO_2 with 10% current increase after 15 min of exposure (Figure 11c, inset). They attributed this exquisite sensitivity to the residence of the charge carriers on the top surface of the nanowires.

Figure 11. (a) SEM image of the transferred nanowires on plastic; (b) Schematic image of nanowire field-effect sensor on plastic; (c) Electrical response of a nanowire array sensor to 20 ppm (red curve), 2 ppm (blue curve), 200 ppb (green curve) and 20 ppb (black curve) NO_2 diluted in N_2 . Inset: an extended response of the sensor to 20 ppb NO_2 [21].



4. Conclusions and Outlook

1D nanostructure field-effect sensors have obvious advantages of high sensitivity, rapid response, small size, room-temperature operation without heating sources, and compatibility with microelectronic integrated circuits. They provide unique amplification strategies to push the LOD to lower levels. More importantly, they provide a way to overcome the big challenge of semiconductor sensors in gas

identification. Some efforts have been done for promoting the practical application of 1D nanostructure field-effect sensors, but only a few 1D nanostructure field-effect sensors have been reported until now, and some critical issues still need to be resolved as follows:

(i) Nanoscaled device fabrication methods.

Most 1D nanostructure sensors apply a two-terminal resistor configuration, which has advantages of simple fabrication and facile measurements. The field-effect devices based on 1D nanostructures are difficult to produced due to the lack of the nanodevice fabrication techniques, which mainly include focused ion beam (FIB) and electron beam lithography (EBL).

(ii) Low-concentration detection.

Although the LOD can be decreased by combining 1D nanostructures and the field-effect device configurations, the detectable concentration of the most reported sensors cannot meet the requirements of environmental monitoring. For example, NO₂ and SO₂ are two of the most dangerous environmental pollutants, and SO₂ is difficult to detect with a semiconductor sensor. The U.S. Environmental Protection Agency has set the acceptable limit in ambient air at a level of 53 ppb for NO₂ and 500 ppb for SO₂, respectively [5,10]. Only a few sensors have reached such levels (Table 1).

(iii) Gas identification.

Until now, how to achieve selective gas sensing in a highly complex background is still an unresolved problem. Future research should further develop the fabrication technique of the nanoscaled sensors, decrease the LOD of sensors, and improve the recognition capacity for practical applications. Other issues, for example, the standard definition of sensor parameters and testing method, long-term stabilities, as well as calibration of the sensors, should also be considered for the development of 1D nanostructure field-effect sensors.

Acknowledgments

This work is supported by NSFC (51322305, 61376074, 51273036, 61261130092 and 51103018), 2009 National Excellent Doctoral Dissertation Award from China (201024), Ministry of Science and Technology of China (2012CB933703), 111 Project (B13013), and Fundamental Research Funds for the Central Universities (12SSXM001).

Conflicts of Interest

The authors declare no conflict of interest.

References

1. Arafat, M.M.; Dinan, B.; Akbar, S.A.; Haseeb, A.S.M.A. Gas sensors based on one dimensional nanostructured metal-oxides: A review. *Sensors* **2012**, *12*, 7207–7258.
2. Afzal, A.; Cioffi, N.; Sabbatini, L.; Torsi, L. NO_x sensors based on semiconducting metal oxide nanostructures: Progress and perspectives. *Sens. Actuators B Chem.* **2012**, *171–172*, 25–42.

3. Li, C.; Zhang, D.; Liu, X.; Han, S.; Tang, T.; Han, J.; Zhou, C. In₂O₃ nanowires as chemical sensors. *Appl. Phys. Lett.* **2003**, *82*, 1613–1615.
4. Torsi, L.; Magliulo, M.; Manoli, K.; Palazzo, G. Organic field-effect transistor sensors: A tutorial review. *Chem. Soc. Rev.* **2013**, *42*, 8612–8628.
5. Shaymurat, T.; Tang, Q.; Tong, Y.; Dong, L.; Liu, Y. Gas dielectric transistor of cupc single crystalline nanowire for SO₂ detection down to sub-ppm levels at room temperature. *Adv. Mater.* **2013**, *25*, 2269–2273.
6. Zhang, D.; Liu, Z.; Li, C.; Tang, T.; Liu, X.; Han, S.; Lei, B.; Zhou, C. Detection of NO₂ down to ppb levels using individual and multiple In₂O₃ nanowire devices. *Nano Lett.* **2004**, *4*, 1919–1924.
7. Singh, N.; Yan, C.; Lee, P.S. Room temperature CO gas sensing using Zn-doped In₂O₃ single nanowire field effect transistors. *Sens. Actuators B Chem.* **2010**, *150*, 19–24.
8. Zou, X.; Wang, J.; Liu, X.; Wang, C.; Jiang, Y.; Wang, Y.; Xiao, X.; Ho, J.C.; Li, J.; Jiang, C.; *et al.* Rational design of sub-parts per million specific gas sensors array based on metal nanoparticles decorated nanowire enhancement-mode transistors. *Nano Lett.* **2013**, *13*, 3287–3292.
9. Mubeen, S.; Moskovits, M. Gate-tunable surface processes on a single-nanowire field-effect transistor. *Adv. Mater.* **2011**, *23*, 2306–2312.
10. Cai, B.; Zhao, X.; Pei, T.; Toninelli, E.; Tang, Q.; Tong, Y.; Liu, Y. Conductive SnO₂:Sb nanobelts as electrodes for detection of NO₂ in ppb level with ultrahigh sensitivity. *Appl. Phys. Lett.* **2014**, *104*, 073112.
11. Kuang, Q.; Li, Z.; Liu, Y.; Xie, Z.; Zheng, L.; Wang, Z. Enhancing the photon- and gas-sensing properties of a single SnO₂ nanowire based nanodevice by nanoparticle surface functionalization. *J. Phys. Chem. B* **2008**, *112*, 11539–11544.
12. Wu, J.M. A room temperature ethanol sensor made from p-type Sb-doped SnO₂ nanowires. *Nanotechnology* **2010**, *21*, 235501.
13. Fan, Z.; Wang, D.; Chang, P.C.; Tseng, W.Y.; Lu, J.G. ZnO nanowire field-effect transistor and oxygen sensing property. *Appl. Phys. Lett.* **2004**, *85*, 5923–5925.
14. Fan, Z.; Lu, J.G. Gate-refreshable nanowire chemical sensors. *Appl. Phys. Lett.* **2005**, *86*, 123510.
15. Liao, L.; Zhang, Z.; Yan, B.; Zheng, Z.; Bao, Q.L.; Wu, T.; Li, C.M.; Shen, Z.X.; Zhang, J.X.; Gong, H.; *et al.* Multifunctional CuO nanowire devices: P-type field effect transistors and CO gas sensors. *Nanotechnology* **2009**, *20*, 085203.
16. Qi, P.; Vermesh, O.; Grecu, M.; Javey, A.; Wang, Q.; Dai, H.; Peng, S.; Cho, K. Toward large arrays of multiplex functionalized carbon nanotube sensors for highly sensitive and selective molecular detection. *Nano Lett.* **2003**, *3*, 347–351.
17. Chang, Y.W.; Oh, J.S.; Yoo, S.H.; Choi, H.H.; Yoo, K.H. Electrically refreshable carbon-nanotube-based gas sensors. *Nanotechnology* **2007**, *18*, 435504.
18. Zhang, J.; Boyd, A.; Tselev, A.; Paranjape, M.; Barbara, P. Mechanism of NO₂ detection in carbon nanotube field effect transistor chemical sensors. *Appl. Phys. Lett.* **2006**, *88*, 123112.
19. Delalande, M.; Clavaguera, S.; Toure, M.; Carella, A.; Lenfant, S.; Deresmes, D.; Vuillaume, D.; Simonato, J.P. Chemical functionalization of electrodes for detection of gaseous nerve agents with carbon nanotube field-effect transistors. *Chem. Commun.* **2011**, *47*, 6048–6050.
20. Kong, J.; Franklin, N.R.; Zhou, C.; Chapline, M.G.; Peng, S.; Cho, K.; Dai, H. Nanotube molecular wires as chemical sensors. *Science* **2000**, *287*, 622–625.

21. McAlpine, M.C.; Ahmad, H.; Wang, D.; Heath, J.R.; Highly ordered nanowire arrays on plastic substrates for ultrasensitive flexible chemical sensors. *Nat. Mater.* **2007**, *6*, 379–384.
22. Du, J.; Liang, D.; Tang, H.; Gao, X. InAs nanowire transistors as gas sensor and the response mechanism. *Nano Lett.* **2009**, *9*, 4348–4351.
23. Zhao, G.; Dong, H.; Jiang, L.; Zhao, H.; Qin, X.; Hu, W. Single crystal field-effect transistors containing a pentacene analogue and their application in ethanol vapor detection. *Appl. Phys. Lett.* **2012**, *101*, 103302.
24. Cid, C.C.; Jimenez-Cadena, G.; Riu, J.; Maroto, A.; Xavier Rius, F.; Batema, G.D.; van Koten, G. Selective detection of SO₂ at room temperature based on organoplatinum functionalized single-walled carbon nanotube field effect transistors. *Sens. Actuators B Chem.* **2009**, *141*, 97–103.
25. Penza, M.; Cassano, G.; Tortorella, F. Gas recognition by activated WO₃ thin-film sensors array. *Sens. Actuators B Chem.* **2001**, *81*, 115–121.
26. Lundström, I.; Shivaraman, S.; Lundkvist, L. A hydrogen-sensitive MOS field-effect transistor. *Appl. Phys. Lett.* **1975**, *26*, 55–56.
27. Lundström, K.I.; Shivaraman, M.S.; Svensson, C.M. A hydrogen sensitive Pd gate MOS transistor. *J. Appl. Phys.* **1975**, *46*, 3876–3881.
28. Ramgir, N.S.; Yang, Y.; Zacharias, M. Nanowire-based sensors. *Small* **2010**, *6*, 1705–1722.
29. Xu, C.; Miura, N.; Yamazoe, N. Grain size effects on gas sensitivity of porous SnO₂-based elements. *Sens. Actuators B Chem.* **1991**, *3*, 147–155.
30. Torsi, L.; Dodabalapur, A. Organic transistors, as discrete elements or implemented in plastic circuits, are challenging, field-effect-based sensing systems. *Anal. Chem.* **2005**, *77*, 380–387.
31. Andringa, A.M.; Meijboom, J.R.; Smits, E.C.P.; Mathijssen, S.G.; Blom, W.M.; Leeuw, D.M. Gate-bias controlled charge trapping as a mechanism for NO₂ detection with field-effect transistors. *Adv. Funct. Mater.* **2011**, *21*, 100–107.
32. Andringa, A.M.; Roelofs, W.S.C.; Sommer, M.; Thelakkat, M.; Kemerink, M.; de Leeuw, D.M. Localizing trapped charge carriers in NO₂ sensors based on organic field-effect transistors. *Appl. Phys. Lett.* **2012**, *101*, 153302.
33. Loiacono, M.J.; Granstrom, E.L.; Frisbie, C.D. Investigation of charge transport in thin, doped sexithiophene crystals by conducting probe atomic force microscopy. *J. Phys. Chem. B* **1998**, *102*, 1679–1688.
34. Vomiero, A.; Bianchi, S.; Comini, E.; Faglia, G.; Ferroni, M.; Sberveglieri, G. Controlled growth and sensing properties of In₂O₃ nanowires. *Cryst. Growth Des.* **2007**, *7*, 2500–2504.
35. Choi, S.W.; Jung, S.H.; Kim, S.S. Functionalization of selectively grown networked SnO₂ nanowires with Pd nanodots by γ -ray radiolysis. *Nanotechnology* **2011**, *22*, 225501.
36. Law, M.; Kind, H.; Messer, B.; Kim, F.; Yang, P. Photochemical sensing of NO₂ with SnO₂ nanoribbon nanosensors at room temperature. *Angew. Chem. Int. Ed.* **2002**, *41*, 2405–2408.
37. Shen, Y.; Yamazaki, T.; Liu, Z.; Meng, D.; Kikuta, T. Hydrogen sensors made of undoped and Pt-doped SnO₂ nanowires. *J. Alloys Compd.* **2009**, *488*, L21–L25.
38. Tien, L.C.; Sadik, P.W.; Norton, D.P.; Voss, L.F.; Pearton, S.J.; Wang, H.T.; Kang, B.S.; Ren, F.; Jun, J.; Lin, J. Hydrogen sensing at room temperature with Pt-coated ZnO thin films and nanorods. *Appl. Phys. Lett.* **2005**, *87*, 222106.

39. Zhang, Y.; Zheng, Z.; Yang, F. Highly sensitive and selective alcohol sensors based on Ag-doped In_2O_3 . *Ind. Eng. Chem. Res.* **2010**, *49*, 3539–3543.
40. Hu, P.; Du, G.; Zhou, W.; Cui, J.; Lin, J.; Liu, H.; Liu, D.; Wang, J.; Chen, S. Enhancement of ethanol vapor sensing of TiO_2 nanobelts by surface engineering. *ACS Appl. Mater. Interfaces* **2010**, *2*, 3263–3269.
41. Joshi, R.K.; Kruis, F.E. Influence of Ag particle size on ethanol sensing of $\text{SnO}_{1.8}$:Ag nanoparticle films a method to develop parts per billion level gas sensors. *Appl. Phys. Lett.* **2006**, *89*, 153116.
42. Kandoi, S.; Gokhale, A.A.; Grabow, L.C.; Dumesic, J.A.; kakis, M.M. Why Au and Cu are more selective than Pt for preferential oxidation of CO at low temperature. *Catal. Lett.* **2004**, *93*, 93–100.
43. Haruta, M. Gold as a novel catalyst in the 21st century preparation, working mechanism and applications. *Gold Bull.* **2004**, *37*, 27–36.
44. Schubert, M. CO oxidation over supported gold catalysts—“Inert” and “Active” support materials and their role for the oxygen supply during reaction. *J. Catal.* **2001**, *197*, 113–122.
45. Kolmakov, A.; Moskovits, M. Functionalizing nanowires with catalytic nanoparticles for gas sensing application. *J. Nanosci. Nanotechnol.* **2008**, *8*, 111–121.
46. Kolmakov, A.; Klenov, D.O.; Moskovits, M. Enhanced gas sensing by individual SnO_2 nanowires and nanobelts functionalized with Pd catalyst particles. *Nano Lett.* **2005**, *5*, 667–673.
47. Star, A.; Joshi, V.; Skarupo, S.; Thomas, D.; Gabriel, J.P. Gas sensor array based on metal-decorated carbon nanotubes. *J. Phys. Chem. B* **2006**, *110*, 21014–21020.
48. Zhang, M.; Su, H.C.; Rheem, Y.; Hangarter, C.M.; Myung, N.V. A rapid room-temperature NO_2 sensor based on tellurium-SWNT hybrid nanostructures. *J. Phys. Chem. C* **2012**, *116*, 20067–20074.
49. Yao, K.; Caruntu, D.; Wozny, S.; Huang, R.; Ikuhara, Y.H.; Cao, B. Towards one key to one lock: Catalyst modified indium oxide nanoparticle thin film sensor array for selective gas detection. *J. Mater. Chem.* **2012**, *22*, 7308–7313.
50. Yu, J.H.; Choi, G.M. Electrical and CO gas-sensing properties of ZnO/SnO_2 hetero-contact. *Sens. Actuators B Chem.* **1999**, *61*, 59–67.
51. Paska, Y.; Stelzner, T.; Christiansen, S.; Haick, H. Enhanced sensing of nonpolar volatile organic compounds by silicon nanowire field effect transistors. *ACS Nano* **2011**, *5*, 5620–5626.
52. Paska, Y.; Stelzner, T.; Assad, O.; Tisch, U.; Christiansen, S.; Haick H. Molecular gating of silicon nanowire field-effect transistors with nonpolar analytes. *ACS Nano* **2012**, *6*, 335–345.
53. Bashouti, M.Y.; Tung, R.T.; Haick, H. Tuning the electrical properties of Si nanowire field-effect transistors by molecular engineering. *Small* **2009**, *5*, 2761–2769.
54. Paska, Y.; Haick, H. Interactive effect of hysteresis and surface chemistry on gated silicon nanowire gas sensors. *ACS Appl. Mater. Interfaces* **2012**, *4*, 2604–2617.
55. Ermanok, R.; Assad, O.; Zigelboim, K.; Wang, B.; Haick, H. Discriminative power of chemically sensitive silicon nanowire field effect transistors to volatile organic compounds. *ACS Appl. Mater. Interfaces* **2013**, *5*, 11172–11183.
56. Wang, B.; Cancilla, J.C.; Torrecilla, J.S. Haick, H. Artificial sensing intelligence with silicon nanowires for ultrasensitive detection in the gas phase. *Nano Lett.* **2014**, *14*, 933–938.
57. Wang, B.; Haick, H. Effect of functional groups on the sensing properties of silicon nanowires toward volatile compounds. *ACS Appl. Mater. Interfaces* **2013**, *5*, 2289–2299.

58. Wang, B.; Haick, H. Effect of chain length on the sensing of volatile organic compounds by means of silicon nanowires. *ACS Appl. Mater. Interfaces* **2013**, *5*, 5748–5756.
59. Ahn, M.-W.; Park, K.-S.; Heo, J.-H.; Park, J.-G.; Kim, D.-W.; Choi, K.J.; Lee, J.-H.; Hong, S.-H. Gas sensing properties of defect-controlled ZnO-nanowire gas sensor. *Appl. Phys. Lett.* **2008**, *93*, 263103.
60. Data Sheet, the MiCS-2714 is a Compact MOS Sensor. Available online: http://www.sgxsensortech.com/site/wp-content/uploads/2013/03/1107_Datasheet-MiCS-2714.pdf (accessed on 23 July 2014).
61. Valentini, L.; Armentano, I.; Kenny, J.M.; Cantalini, C.; Lozzi, L.; Santucci, S. Sensors for sub-ppm NO₂ gas detection based on carbon nanotube thin films. *Appl. Phys. Lett.* **2003**, *82*, 961–963.

© 2014 by the authors; licensee MDPI, Basel, Switzerland. This article is an open access article distributed under the terms and conditions of the Creative Commons Attribution license (<http://creativecommons.org/licenses/by/3.0/>).